$Si_{1-x-y}Ge_xC_y$ alloy band structures by linear combination of atomic orbitals

B. A. Orner[a] and J. Kolodzey
Department of Electrical Engineering, University of Delaware, Newark, Delaware 19716

(Received 24 October 1996; accepted for publication 7 February 1997)

We have applied a virtual crystal approximation to the linear combination of atomic orbitals method to calculate critical point energies of unstrained $Si_{1-x-y}Ge_xC_y$ alloys spanning the composition parameter space. Additionally, we have calculated the band structure across the Brillouin zone for a series of alloy compositions. We found the band energies had significant bowing departures from linearity throughout the system. In some cases, the energy band gap was not monotonically dependent on composition. Our theoretical results are compared with recent experimental results, and good agreement was found overall. © *1997 American Institute of Physics.* [S0021-8979(97)05010-X]

I. INTRODUCTION

The $Si_{1-x-y}Ge_xC_y$ alloy system is being investigated for use in group IV heterostructure devices.[1–5] At certain compositions, the system is lattice matched to Si, and could potentially be lattice matched to 3C-SiC. It could further be useful in lattice mismatched devices fabricated on Ge or diamond substrates, for example, or as a virtual substrate for other materials.

Usually, the ultimate motivation to explore new materials is to exploit a property of an alloy band structure that is not attainable using pure elements, such as band offsets in a lattice matched heterostructure, or an intrinsic property of the band structure such as lighter carrier effective mass. The band structure of group IV alloys, however, is largely unknown.

Because alloys containing C are metastable,[6] they cannot be produced by simple high temperature mixing. Several groups have recently produced crystalline random alloys with under 5% C using techniques such as molecular beam epitaxy or chemical vapor deposition.[7–9] Even for these C lean binary and ternary alloys, experimental band gap data are sparse. As the alloy materials are difficult to produce and analyze, a comprehensive experimental study across the whole composition range has not yet been completed.

For this reason, theoretical predictions of alloy band structure are useful first steps toward device design. Theoretical studies of the band structure of this alloy system have focused on $Si_{1-x}Ge_x$ and $Si_{1-y}C_y$ binary alloys, though a few ternary alloys have been studied.[10–12] Linear interpolation of critical points using the elemental values as endpoints yields a straightforward description of the band gap of any particular composition.[12] First principle calculations of $Si_{1-y}C_y$ alloys[10,13,14] have been incongruent with such a linear interpolation, predicting decreases in the band gap as C content is increased, and semimetallic materials at some compositions. These methods predicted the magnitude of this decrease to be between -20 and -100 meV/% C.

The first principles nature of these calculations is appealing, and the intriguing results have increased interest in the band structure of these alloys. These previous calculations, however, performed by the plane wave techniques,[13] *GW*,[14] and linear muffin tin orbital (LMTO)[10] methods, do have some drawbacks.

For example, previous calculations employed a supercell approach in which individual Si, Ge, and C atoms in appropriate proportions were located on diamond lattice sites to simulate the random alloy. The alloy composition is thus limited to discrete points in composition parameter space. The composition interval spacing is limited by the number of atoms in the supercell (in the referenced work, interval spacing was usually 12.5%). Our approach employs a virtual crystal approximation (VCA) within the linear combination of atomic orbitals (LCAO) method. This permits band structure calculations for alloys of arbitrary composition. A similar approach has been applied to $Si_{1-x}Ge_x$ alloys[15,16] but to our knowledge has not been applied to group IV semiconductor alloys containing C. As a future research subject, empirical pseudo-potential band structure calculations could be performed by a similar interpolation of parameters.

Furthermore, due to the fairly formidable calculations, only a few compositions were reported, primarily Si rich $Si_{1-y}C_y$ alloys. The LCAO calculations employed herein were accomplished for 1250 compositions.

Finally, the calculations generally (except for the *GW*[14] results) fail to accurately predict experimental band gap energies at the elemental end points, and are therefore questionable for conclusions on alloy properties. They are most useful in predicting trends in the band gap as composition is varied. To obtain absolute values for the band gap energies, an *ad hoc* correction factor must be included. If this correction factor is linearly interpolated to obtain alloy corrections, departures from linearity could give unexpected results. Due to the semiempirical nature of the LCAO method, the band structure at the elemental endpoints agree well with experimental values, and no correction factors were required.

II. THEORETICAL APPROACH

Our approach, like all methods, involves some assumptions and limitations. The VCA technique we employ does not account for localized strain effects resulting from a dis-

[a]Electronic mail:orner@ee.udel.edu

parity in bond lengths between Si, Ge, and C. The smaller C atomic radius is expected to alter both the bond angles and lengths, resulting in a deviation from the ideal diamond crystal structure. Previous articles have reported that this departure decreases the energy band gap of these alloys.[11,13] The extent to which this effect decreases the band gap is not established. In this article we demonstrate that a VCA produces a large bowing departure in the band gap-composition relation. Combined with other studies, this may clarify the extent to which localized strain decreases the band gap.

Similarly, the VCA does not account for band broadening due to alloy disorder. This broadening can reduce the effective band gap energy and other transition energies. Techniques such as the coherent potential approximation (CPA)[17–19] do account for alloy disorder. The role of alloy disorder in $Si_{1-x-y}Ge_xC_y$ alloys has not been established. In the $Si_{1-x}Ge_x$ system, CPA studies[18,19] have found that disorder reduced the band gap energy by at most 7 meV, thus the CPA band gap energy differed only slightly from the VCA band gap energy. These studies did find larger band broadening further from the band edge, however, and cautioned that the extent of broadening could differ for other alloy systems. The VCA results presented here provide an initial point of information on the band structure of a wide range of $Si_{1-x-y}Ge_xC_y$ alloys. Comparison of these VCA results with future CPA studies will be of value in studies of alloy disorder band broadening in $Si_{1-x-y}Ge_xC_y$.

Therefore, we feel there is merit to exploring the band structure of this alloy system by several methods, and the approach taken herein is intended to complement previous work. This will allow for comparison between the results of a wide variety of different techniques. We do not claim the approach we employ is superior, but rather that, in light of sparse and inconsistent experimental data, many alternative theoretical and experimental approaches should be explored.

The LCAO formalism employed here is a modified version[20] of the classic work of Slater and Koster.[21] We use a three-center, third nearest-neighbor Hamiltonian. Traditionally, an orthogonal hybridized atomic orbital basis is assumed, with any non-orthogonality being absorbed by the empirical Slater-Koster (SK) parameters. We have performed our calculations by this traditional orthogonal LCAO method, but have also repeated some calculations using a non-orthogonal LCAO method.[22] For this, we formulated a separate overlap matrix with a separate set of empirical parameters to account for non-orthogonality. The Schroedinger equation in the non-orthogonal case is solved by

$$|S^{-1/2}HS^{-1/2}-EI|=0, \tag{1}$$

where H is an 8×8 Hamiltonian parameter matrix, S is an 8×8 overlap matrix, and E is the set of eigenvalues which solve the Schroedinger equation. In the orthogonal LCAO formulation, S is taken as the identity matrix. We focus initially and primarily on the results from the orthogonal method, due to the smaller parameter set involved. Limited results from the non-orthogonal method are also presented. The Hamiltonian matrix elements for the diamond structure, including third nearest neighbors[20,21] are listed in Table I.

Twenty empirical parameters were required for the orthogonal formulation, and 38 parameters were required for the non-orthogonal formulation. For the elemental end points we used those of Papaconstantopoulos,[20] which were obtained by curve fitting to pseudo-potential band structures.

Careful consideration must be given to the size of the empirical parameter set. A large parameter set permits excellent agreement between the band structure calculations and experimental results for the elemental end points. However, with larger parameter sets, it becomes difficult to obtain physically meaningful values for the SK parameters through curve fitting. This limits the confidence in the interpolated values to some extent—presumably any decrease in accuracy would be most pronounced for alloys in which no single element is the dominant component. We feel this fact is mitigated by the improved accuracy at and near the end points, and have thus employed larger parameter sets. Normally, accuracy is rapidly lost if fewer than 20 parameters are employed. By using a 10×10 matrix, Vogl *et al.*[23] have reduced the number of parameters to eight and have achieved good results, though the formulation we have employed still gives an improved representation of the band structure as evidenced by the superior experimental agreement of energies at the critical points.

The alloy SK parameters were obtained by interpolation, using the elemental SK parameters as end points. The on-site SK parameters were linearly interpolated with composition. The parameters for the first, second, and third nearest neighbors (for S as well as H) were interpolated in accordance with Harrison's d^{-2} rule:[23,24]

$$E_{\text{alloy}}=\left(\sum_{i=\text{Si,Ge,C}} d_i x_i\right)^{-2} \sum_{i=\text{Si,Ge,C}} (d_i)^2 x_i E_i, \tag{2}$$

where E_{alloy} and E_i are a particular empirical SK parameter for the alloy and elemental end points, respectively, and d_i is the appropriate nth nearest neighbor distance in crystalline Si, Ge, or C. Finally, x_i is the atomic fraction of each alloy component. The first term represents the nth nearest neighbor distance in the alloy. Here we have assumed Vegard's law is followed for these alloys, and have obtained the neighbor distances by linear interpolation.

After obtaining the set of SK parameters for an alloy, the eigenvalues were found by diagonalizing and solving Eq. (1) for a given wave vector **k**. To study the composition dependence of the critical points, the eigenvalues were obtained at the Γ and L symmetry points, and for 15 values of **k** on the Δ axis between $(2\pi/a)(0.7)[001]$ and $(2\pi/a)(0.95)[001]$ to obtain the Δ minimum. For selected alloys, the band structure was obtained by evaluating Eq. (1) on a grid of 100 **k** values.

III. RESULTS AND DISCUSSION

Using the orthogonal method, the composition dependence of the Γ, Δ, and L conduction band minima for each of the unstrained binary systems is indicated in Figs. 1–3. Nonlinear behavior was observed for all three binary systems, but was not pronounced for the $Si_{1-x}Ge_x$ system, for which we have compared the theoretical band gap to the

TABLE I. Matrix elements for the H and S matrices. The H and S matrix elements have the same form and differ only by their empirical constants. On-site, first, second, and third nearest neighbors of the diamond lattice structure are included. Matrix elements H are described by a set of orbitals (s, x, or y) and numbers indicating the atomic site on the two-atom diamond basis. Wave vector $\mathbf{k}$ is expressed in units of $2\pi/a$, where a is the alloy lattice constant. Each empirical parameter E is designated by two letters indicating the two hybridized atomic orbitals of $\langle \Psi_1 | H | \Psi_2 \rangle$ and a number indicating the distance and direction (where distinct) between the atomic centers. Here sx indicates an s orbital and any p orbital (x, y, or z) xx indicates two p orbitals of equal magnetic quantum numbers, and xy indicates two p orbitals with differing magnetic quantum numbers.

$$H_{s1/s1}=H_{s2/s2}=E_{ss}(000)+4E_{ss}(220)[\cos(k_x)\cos(k_y)+\cos(k_y)\cos(kz)+\cos(k_x)\cos(k_z)].$$

$$H_{x1/x1}=H_{x2/x2}=E_{xx}(000)+4E_{xx}(220)[\cos(k_x)\cos(k_y)+\cos(k_x)\cos(k_z)]+4E_{xx}(022)\cos(k_y)\cos(k_z).$$

$$\begin{aligned}H_{s1/s2}=H^*_{s2/s1}=&4E_{ss}(111)\cos\left(\frac{k_x}{2}\right)\cos\left(\frac{k_y}{2}\right)\cos\left(\frac{k_z}{2}\right)\\&+4E_{ss}(311)\left[\cos\left(\frac{k_x}{2}\right)\cos\left(\frac{k_y}{2}\right)\cos\left(\frac{k_z}{2}\right)+\cos\left(\frac{k_y}{2}\right)\cos\left(\frac{k_x}{2}\right)\cos\left(\frac{k_z}{2}\right)+\cos\left(\frac{k_z}{2}\right)\cos\left(\frac{k_x}{2}\right)\cos\left(\frac{k_y}{2}\right)\right]\\&-i4E_{ss}(111)\sin\left(\frac{k_x}{2}\right)\sin\left(\frac{k_y}{2}\right)\sin\left(\frac{k_z}{2}\right)\\&+i4E_{ss}(311)\left[\sin\left(\frac{k_x}{2}\right)\sin\left(\frac{k_y}{2}\right)\sin\left(\frac{k_z}{2}\right)+\sin\left(\frac{k_y}{2}\right)\sin\left(\frac{k_x}{2}\right)\sin\left(\frac{k_z}{2}\right)+\sin\left(\frac{k_z}{2}\right)\sin\left(\frac{k_x}{2}\right)\sin\left(\frac{k_y}{2}\right)\right].\end{aligned}$$

$$\begin{aligned}H_{s1/x2}=-H^*_{s2/x1}=&4E_{sx}(111)\cos\left(\frac{k_x}{2}\right)\sin\left(\frac{k_y}{2}\right)\sin\left(\frac{k_z}{2}\right)\\&-4E_{sx}(311)\cos\left(\frac{k_x}{2}\right)\sin\left(\frac{k_y}{2}\right)\sin\left(\frac{k_z}{2}\right)\\&-4E_{sx}(113)\cos\left(\frac{k_x}{2}\right)\left[\sin\left(\frac{k_y}{2}\right)\sin\left(\frac{k_z}{2}\right)+\sin\left(\frac{k_z}{2}\right)\sin\left(\frac{k_y}{2}\right)\right]\\&-i4E_{sx}(111)\sin\left(\frac{k_x}{2}\right)\cos\left(\frac{k_y}{2}\right)\cos\left(\frac{k_z}{2}\right)\\&-i4E_{sx}(311)\sin\left(\frac{k_x}{2}\right)\cos\left(\frac{k_y}{2}\right)\cos\left(\frac{k_z}{2}\right)\\&-i4E_{sx}(113)\sin\left(\frac{k_x}{2}\right)\left[\cos\left(\frac{k_y}{2}\right)\cos\left(\frac{k_z}{2}\right)+\cos\left(\frac{k_z}{2}\right)\cos\left(\frac{k_y}{2}\right)\right].\end{aligned}$$

$$H_{s1/x1}=-H^*_{s2/x2}=-4E_{sx}(022)\sin(k_y)\sin(k_z)+i4E_{sx}(220)[\sin(k_x)\cos(k_y)+\sin(k_x)\cos(k_z)].$$

$$\begin{aligned}H_{x1/x2}=H^*_{x2/x1}=&4E_{xx}(111)\cos\left(\frac{k_x}{2}\right)\cos\left(\frac{k_y}{2}\right)\cos\left(\frac{k_z}{2}\right)\\&+4E_{xx}(311)\left[\cos\left(\frac{k_x}{2}\right)\cos\left(\frac{k_y}{2}\right)\cos\left(\frac{k_z}{2}\right)+\cos\left(\frac{k_y}{2}\right)\cos\left(\frac{k_x}{2}\right)\cos\left(\frac{k_z}{2}\right)+\cos\left(\frac{k_z}{2}\right)\cos\left(\frac{k_x}{2}\right)\cos\left(\frac{k_y}{2}\right)\right]\\&-i4E_{xx}(111)\sin\left(\frac{k_x}{2}\right)\sin\left(\frac{k_y}{2}\right)\sin\left(\frac{k_z}{2}\right)\\&+i4E_{xx}(311)\left[\sin\left(\frac{k_x}{2}\right)\sin\left(\frac{k_y}{2}\right)\sin\left(\frac{k_z}{2}\right)+\sin\left(\frac{k_y}{2}\right)\sin\left(\frac{k_x}{2}\right)\sin\left(\frac{k_z}{2}\right)+\sin\left(\frac{k_z}{2}\right)\sin\left(\frac{k_x}{2}\right)\sin\left(\frac{k_y}{2}\right)\right].\end{aligned}$$

$$\begin{aligned}H_{x1/y2}=H^*_{x2/y1}=H_{y1/x2}&-4E_{xy}(111)\sin\left(\frac{k_x}{2}\right)\sin\left(\frac{k_y}{2}\right)\cos\left(\frac{k_z}{2}\right)\\&+4E_{xy}(113)\cos\left(\frac{k_z}{2}\right)\sin\left(\frac{k_x}{2}\right)\sin\left(\frac{k_y}{2}\right)\\&+4E_{xy}(311)\cos\left(\frac{k_z}{2}\right)\left[\sin\left(\frac{k_x}{2}\right)\sin\left(\frac{k_y}{2}\right)+\sin\left(\frac{k_y}{2}\right)\sin\left(\frac{k_x}{2}\right)\right]\\&+i4E_{xy}(111)\cos\left(\frac{k_x}{2}\right)\cos\left(\frac{k_y}{2}\right)\sin\left(\frac{k_z}{2}\right)\\&+4E_{xy}(113)\sin\left(\frac{k_z}{2}\right)\cos\left(\frac{k_x}{2}\right)\cos\left(\frac{k_y}{2}\right)\\&+i4E_{xy}(311)\sin\left(\frac{k_z}{2}\right)\left[\cos\left(\frac{k_x}{2}\right)\cos\left(\frac{k_y}{2}\right)+\cos\left(\frac{k_y}{2}\right)\cos\left(\frac{k_x}{2}\right)\right].\end{aligned}$$

$$H_{x1/y1}=H^*_{x2/y2}=-4E_{xy}(220)\sin(k_x)\sin(k_y)-i4E_{xy}(022)[\cos(k_x)\sin(k_z)-\cos(k_y)\sin(k_z)].$$

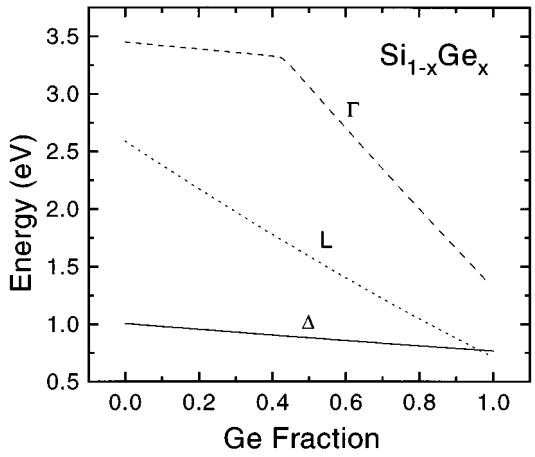

FIG. 1. Composition dependence of $Si_{1-x}Ge_x$ alloy critical points as calculated by the orthogonal LCAO method. The dependence is predominately linear. The Δ-L crossover occurs at $x=0.96$. The nonlinearity in the Γ critical point arises from a crossover to an eigensolution of differing symmetry near $x=0.4$.

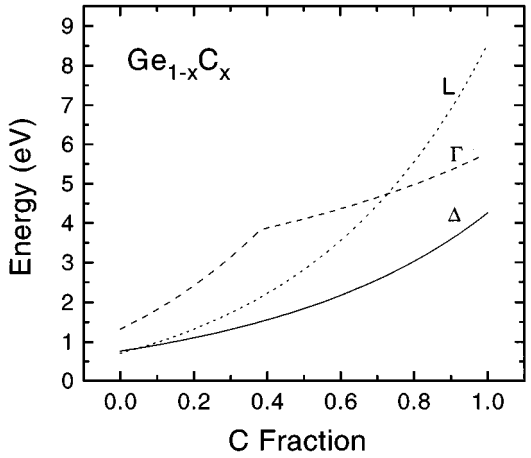

FIG. 3. Composition dependence of $Ge_{1-y}C_y$ alloy critical points as calculated by the orthogonal LCAO method. Significant nonlinearities are evident. Crossover from a L to Δ minimum is indicated for $x=0.05$.

experimental band gap (Fig. 4). Agreement is generally good, though the Δ to L crossover is predicted to occur at about 4% Si rather than the experimental value of 15%,[25] and our theory underestimates the band gap of Si. For the $Ge_{1-y}C_y$ system (Fig. 3), crossover from an L to a Δ point minimum at 5% C is predicted. The sublinear bowing departure for this system is significant—for $x<0.2$ we predict an L point dependence of 29.6 meV/% C and a Δ point dependence of 16.7 meV/% C, whereas a linear interpolation would give 78.2 and 34.9 meV/% C, respectively. For the $Si_{1-y}C_y$ system, we predict a Δ point minimum throughout the system with a composition dependence of 16.7 meV/% C for Si rich samples, rather than a linear value of 32.5 meV/% C.

Fig. 5 gives the band gap-composition dependence for a range of unstrained $Si_{1-x-y}Ge_xC_y$ alloys ($y<0.10$), which may be compared with experimental results. If measurements were obtained from relaxed alloys, a direct comparison may be made. However, in many cases, measurements were performed on thin strained alloys grown on Si substrates. In these cases, a deformation potential must be applied to remove the effects of strain on the band structure.[7,26] Because the deformation potentials for these alloys are unknown, such approaches have relied on the assumption that the deformation potentials are similar to those of Si or $Si_{1-x}Ge_x$.

Our results are compared with theoretical and experimental results of other workers in Table II. For our orthogonal LCAO calculations a dependence of 16.7 meV/% C for Δ minima and 29.6 meV/% C for L minima was predicted. Overall, a large disparity exists between the results of various workers. Some of these differences could be attributed to composition and temperature differences as well as unexpected strain behavior, but inconsistencies exist even after

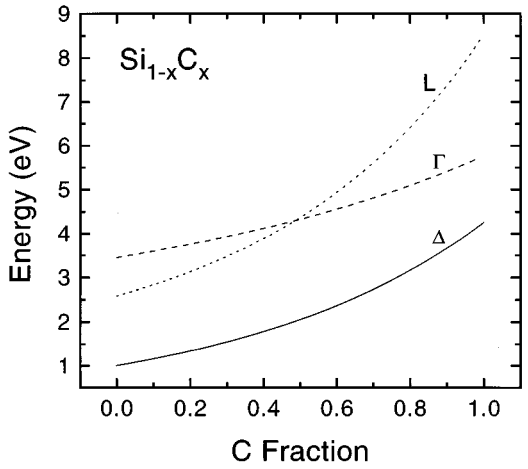

FIG. 2. Composition dependence of $Si_{1-y}C_y$ alloy critical points as calculated by the orthogonal LCAO method. The relation is nonlinear for all three critical points. A Δ minimum is indicated throughout this alloy system.

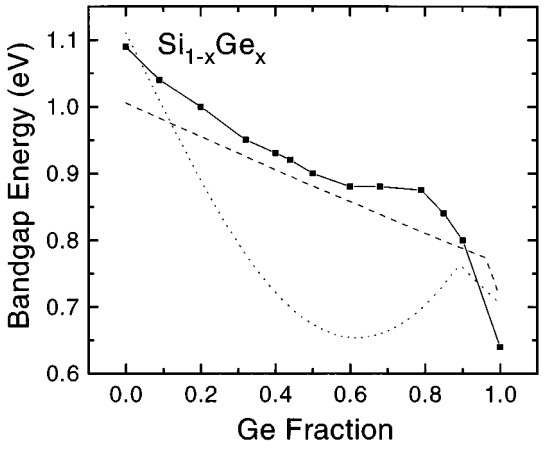

FIG. 4. Composition dependence of the $Si_{1-x}Ge_x$ band gap energy. Experimental data (see Ref. 36) is indicated by the solid line. The dashed line indicates the results of our orthogonal LCAO calculations, and the dotted line indicates the results of our nonorthogonal LCAO calculations.

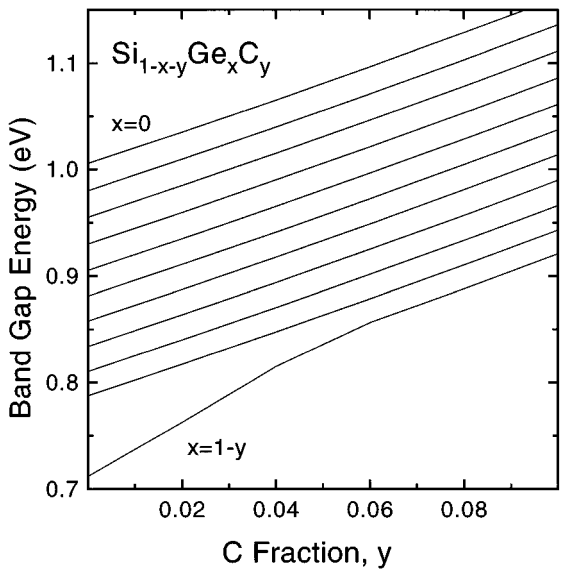

FIG. 5. Variation of the band gap energy as C is added to $Si_{1-x}Ge_x$ alloys. The top and bottom lines represent $Si_{1-y}C_y$ and $Ge_{1-y}C_y$ binary alloys, respectively. The lines represent ternary alloys of composition ratios, $x/(1-y)$, which increase in increments of 0.1 from 0 at the top to 1 at the bottom ($y \neq 1$).

considering these factors. Our LCAO results for both Δ and L minima agree well with experimental absorption results for ternary alloys, though a somewhat higher value of 63 meV/% C was experimentally found for $Ge_{1-y}C_y$ alloys. We do not obtain agreement, however, with photoluminescence (PL) and multiple quantum well (MQW) PL results for Si rich alloys, most of which indicate a variation of −7 to −19 meV/% C. Perhaps the values assumed for the deformation potential incorrectly predict the strain-free behavior. Alternatively, localized strain and alloy disorder effects, which we have not considered, could account for this decrease.

Our LCAO results for the E_1 critical point energy are in excellent agreement with spectroscopic ellipsometry results for $Si_{1-y}C_y$. The E_1 critical point energy is associated with direct transitions near the L point.[25,32] Spectroscopic ellipsometry indicates a 43 meV/% C composition dependence after strain effects are considered,[26,33,34] and our calculations predict a 40 meV/% C composition dependence. Finally, we predict a band gap energy of 2.053 eV for $Si_{0.5}C_{0.5}$, which agrees fairly well with the observed 3C-SiC band gap of 2.25 eV.[25] By comparison, the first principles calculations predict a band gap of at most 1.3 eV.[10,11,14]

By assuming Vegard's law holds for the lattice constant, and therefore alloys with a Ge:C ratio of 8:1 are lattice matched to Si, we plot the predicted band gap of the Si lattice matched $Si_{1-x-y}Ge_xC_y$ alloys in Fig. 6. We find little variation in the band gap among these alloys, however, $Si_{1-x-y}Ge_xC_y$/Si band offsets may still exist. Additionally, the band gap may be modified through strain, perhaps with greater flexibility than the $Si_{1-x}Ge_x$ system.

Fig. 7 is a band gap contour plot for the $Si_{1-x-y}Ge_xC_y$ system, giving the minimum band gaps versus composition. The uneven contour spacing indicates nonlinearities. Soref *et al.* have also found a sublinear increase in the band gap with increasing C for C lean alloys and a rapid band gap

TABLE II. C concentration dependence of the unstrained alloy band gap energy E_G. The upper section of the table shows the results of theoretical calculations; the lower section lists experimental results. The data for the $Ge_{1-y}C_y$ system assumed fully relaxed alloys. The remaining experimental data were collected on strained thin films with various C contents. The authors of these articles have estimated the deformation potentials and calculated the change in the band gap due to strain effects. By accounting for this, the band gap energy dependence on C due to alloying was computed, and is summarized here.

ΔE_G (meV/% C)	$Si_{1-x-y}Ge_xC_y$ Composition	Technique	Source
30	$x>0.96$	Orthogonal LCAO	Current study
17	$x<0.96$, $y\leqslant 0.10$	Orthogonal LCAO	Current study
44	$x=0$	Linear interpolation	[d]
128	$x>0.96$, $y=1-x$	Linear interpolation	[d]
48	$x<0.96$, $y=1-x$	Linear interpolation	[d]
-83	$x=0$, $y\leqslant 0.13$	*Ab inito* pseudo potential	[e]
−100	$x=0$, $y\leqslant 0.13$	*GW*	[f]
−30	$x=0$, $y\leqslant 0.13$	LMTO	[c]
−20	$x=0.125$, $y\leqslant 0.13$	LMTO	[c]
63	$x=1-y$, $y\leqslant 0.03$	Absorption	[g]
45	$x=0.88$, $y\leqslant 0.01$	Absorption	[h]
14	$x=0.08$, $y\leqslant 0.01$	Absorption	[i]
−19	$x=0.24$,$x=0.38$, $y\leqslant 0.011$	PL	[a]
−7	$x=0.15$, $y\leqslant 0.009$	MQW PL	[j]
−19	$x=0$, $y\leqslant 0.016$	MQW PL	[b]
67	$x=0$, $y\leqslant 0.014$	PL	[k]

[a]Reference 7.
[b]Reference 8.
[c]Reference 10.
[d]Reference 12.
[e]Reference 13.
[f]Reference 14.
[g]Reference 27.
[h]Reference 28.
[i]Reference 29.
[j]Reference 30.
[k]Reference 31.

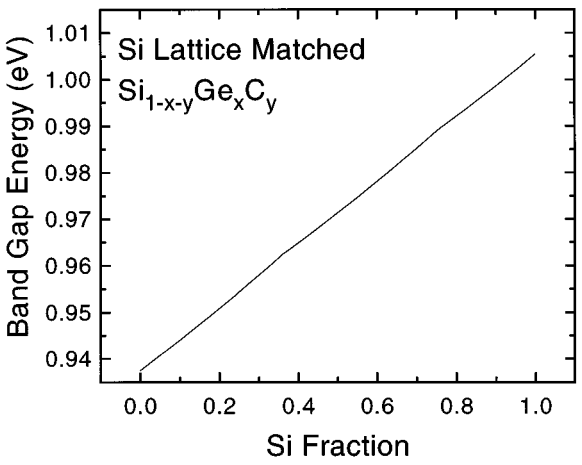

FIG. 6. Band gap energy of Si lattice matched $Si_{1-x-y}Ge_xC_y$ alloys. Vegard's law was employed to calculate the Ge:C ratio (8:1) required for lattice matching.

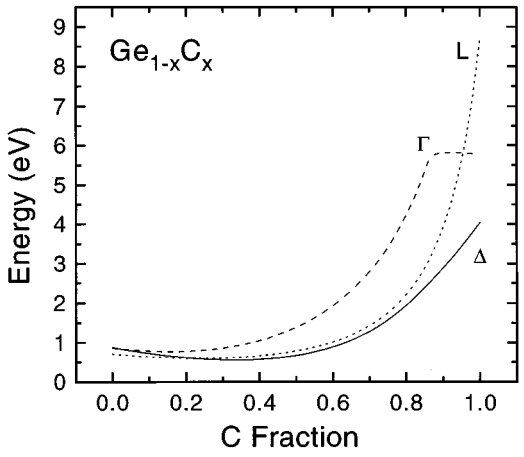

FIG. 8. Critical point energies of the $Ge_{1-y}C_y$ alloy system as calculated by the nonorthogonal LCAO method. Critical point energies are predicted to initially decrease as C is added to Ge, then rise rapidly for C rich alloys.

increase for C rich alloys[35] in a plot obtained by combining LMTO theoretical results for Si rich alloys[10] with experimental results for Ge rich alloys.[9] Because the LMTO results were included, he did find a band gap decrease as C content increased for some Si rich alloys.

The non-orthogonal calculations produced more pronounced nonlinearities. For the Ge rich $Si_{1-x-y}Ge_xC_y$ alloys and $Ge_{1-y}C_y$ alloys (Fig. 8) a decrease in the band gap with increasing C is predicted for some alloys with Δ minimums. $Si_{1-y}C_y$ alloys (Fig. 9) show a decrease only in the L minimum, which is never the conduction band minimum for this system, and thus the band gap of the $Si_{1-y}C_y$ system is indicated by this calculation to be monotonically increasing. Similarly the theoretical $Si_{0.5}C_{0.5}$ band gap energy of 1.608 eV does not agree as well as the orthogonal method. As shown in Fig. 4, the bowing departure that is observed experimentally for the $Si_{1-x}Ge_x$ system is overestimated, indicating a non-monotonic band gap variation that is not experimentally observed.

As expected from the increased number of parameters, the nonorthogonal method produced superior results at the end points but appear to deviate at the midpoints of the interpolation. We consider the orthogonal method to be a better representation of the physical alloy band structure due to its improved match to the experimental band gaps in the $Si_{1-x}Ge_x$ system, and to 3C-SiC. The nonorthogonal method may ultimately provide a superior description of the alloy band structure if an improved parameter set could be found. In principle, experimental results for critical point energies of alloys could be included in the fitting algorithm used to determine the parameter set, and the non-orthogonal LCAO results could then be used to interpolate the band structure

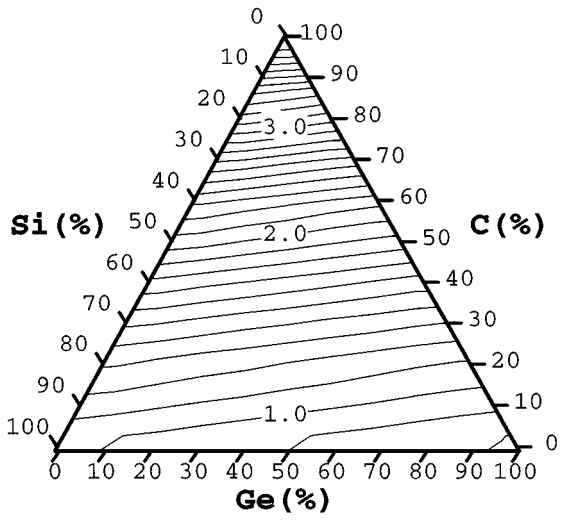

FIG. 7. Contour plot of band gap energies of $Si_{1-x-y}Ge_xC_y$ alloys as calculated by the orthogonal LCAO method. Units for contour labels are eV; each contour line represents a step of 0.1 eV. Uneven contour spacing illustrates nonlinearities, particularly evident for C rich alloys. Band gap energy variations are monotonic with composition.

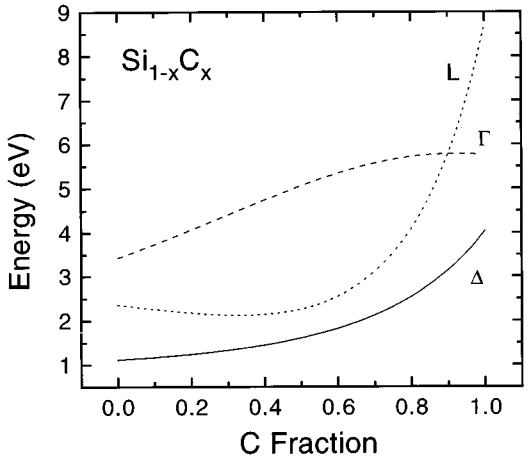

FIG. 9. Critical point energies of the $Si_{1-y}C_y$ system as calculated by the nonorthogonal LCAO method. The L point energy initially decreases as C is added to Si, but the conduction band minimum at Δ increases slightly.

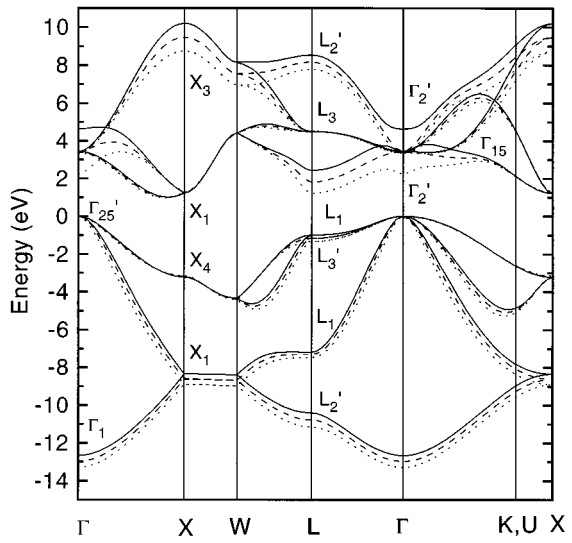

FIG. 10. Band structure of $Si_{1-x-y}Ge_xC_y$ alloys lattice matched to Si calculated by the orthogonal LCAO method. Alloys consisted of 90% Si (solid lines), 50% Si (dashed lines), and 10% Si (dotted lines). The remaining alloy components were Ge and C in an 8:1 ratio. The valance band structure is virtually unchanged. The conduction bands have a similar structure throughout, with the most noticeable changes being a lowering with decreasing Si in energy of the minimums at L and Γ, and a change in symmetry of the conduction band minimum at Γ.

for other wave vectors and other alloys. Presently, experimental data is sparse for alloys containing C.

Complete band structures were calculated for selected alloys using the orthogonal LCAO method. Fig. 10 gives the band structure of a series of lattice matched $Si_{1-x-y}Ge_xC_y$ alloys. Figs. 10–13 give the band structure of several C lean binary and ternary alloys, illustrating changes due to the addition of C. Fig. 14 shows the band structure of a 3C-SiC

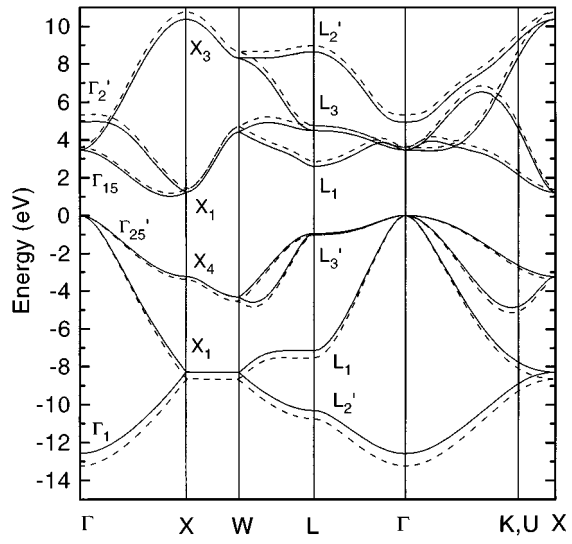

FIG. 11. Band structure of Si (solid lines), and $Si_{0.90}C_{0.10}$ (dashed lines) as calculated by the orthogonal LCAO method. There are no significant changes in the band structure expected other than an increase in the band gap energy with C.

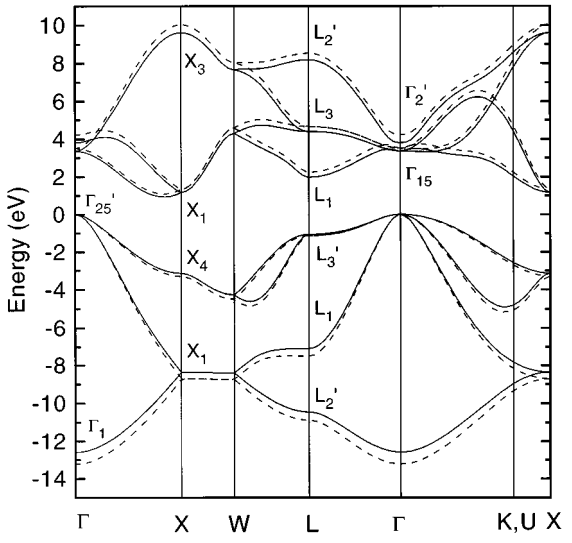

FIG. 12. Band structure of $Si_{0.70}Ge_{0.30}$ (solid lines) and $Si_{0.63}Ge_{0.27}C_{0.10}$ (dashed lines) as calculated by the orthogonal LCAO method.

lattice matched (by Vegard's law) $Ge_{1-y}C_y$ alloy. The resulting band structures vary gradually with composition. In general, alloys with one dominant element had a band structure characteristic of that element. A Δ minimum is expected for most alloys, except those with at least 95% Ge. None of the alloys was predicted to have a direct band gap for any composition.

IV. CONCLUSION

In conclusion, we have calculated the band structure for the $Si_{1-x-y}Ge_xC_y$ alloy system by the empirical LCAO method. An indirect Δ minimum was indicated for most alloys, and the critical point energies were found to have a

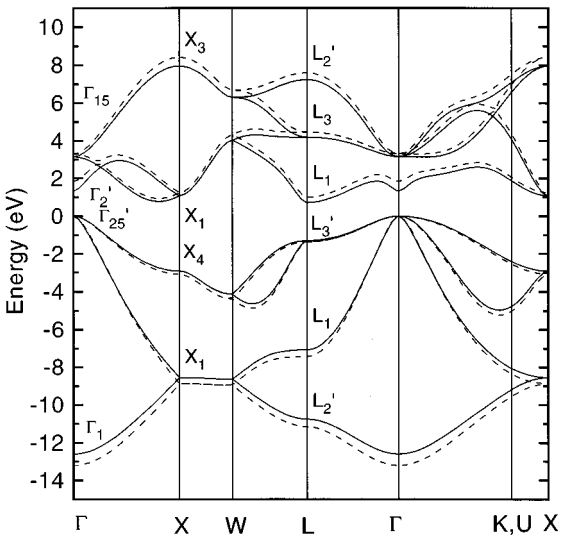

FIG. 13. Band structure of Ge (solid lines) and $Ge_{0.90}C_{0.10}$ (dashed lines) as calculated by the orthogonal LCAO method.

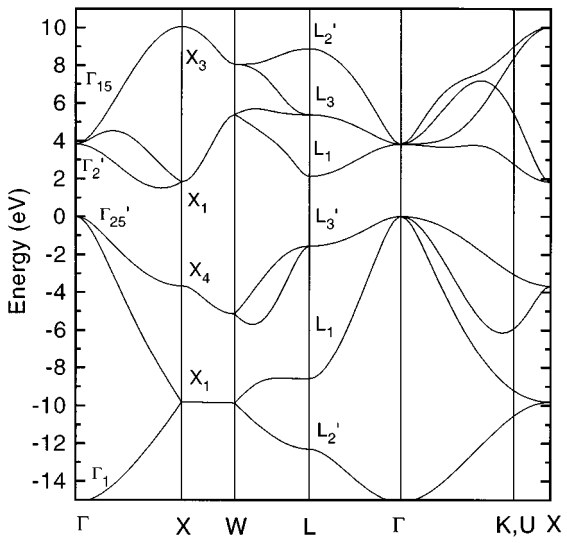

FIG. 14. Band structure of $Ge_{0.62}C_{0.38}$ as calculated by the orthogonal LCAO method. By Vegard's law, this alloy is lattice matched to 3C-SiC.

monotonic but non-linear composition dependence. Our goal was to show results of this band structure approach for comparison with other published calculations.

ACKNOWLEDGMENTS

The authors are grateful to Dr. M. Berding, Dr. P. Christie, and Dr. R. Soref for useful discussions and review of this manuscript. This work was supported by ONR Grant No. N00014-93-1-0393 and DARPA Contract No. F49620-96-C-0006.

[1] J. C. Bean, Proc. IEEE **80**, 571 (1992).
[2] R. A. Soref, Proc. IEEE **81**, 1687 (1993).
[3] H. J. Osten, J. Cryst. Growth **157**, 268 (1995).
[4] K. Eberl, S. S. Iyer, S. Zollner, J. C. Tsang, and F. K. LeGoues, Appl. Phys. Lett. **60**, 3033 (1992).
[5] J. W. Strane, H. J. Stein, S. R. Lee, B. L. Doyle, S. T. Picraux, and J. W. Mayer, Appl. Phys. Lett. **63**, 2786 (1993).
[6] R. I. Scace and G. A. Slack, J. Chem. Phys. **30**, 1551 (1959).
[7] A. St. Amour, C. W. Liu, J. C. Sturm, Y. Lacroix, and M. L. W. Thewalt, Appl. Phys. Lett. **67**, 3915 (1995).
[8] K. Brunner, K. Eberl, and W. Winter, Phys. Rev. Lett. **76**, 303 (1996).
[9] J. Kolodzey, P. R. Berger, B. A. Orner, D. Hits, F. Chen, A. Khan, X. Shao, M. Waite, S. I. Shah, C. P. Swann, and K. M. Unruh, J. Cryst. Growth **157**, 386 (1995).
[10] J. Xie, K. Zhang, and X. Xie, J. Appl. Phys. **77**, 3868 (1995).
[11] M. A. Berding, A. Sher, and M. van Schilfgaarde, Phys. Rev. B (in press).
[12] R. A. Soref, J. Appl. Phys. **70**, 2470 (1991).
[13] A. A. Demkov and O. F. Sankey, Phys. Rev. B **48**, 2207 (1993).
[14] J. Gryko and O. F. Sankey, Phys. Rev. B **51**, 7295 (1995).
[15] K. E. Newman and J. D. Dow, Phys. Rev. B **30**, 1929 (1984).
[16] G. Theodorou, N. D. Vlachos, and C. Tserbak, J. Appl. Phys. **76**, 5294 (1994).
[17] P. Soven, Phys. Rev. **156**, 809 (1967).
[18] D. Stroud and H. Ehreneich, Phys. Rev. B **2**, 3197 (1970).
[19] S. Krishnamurthy, A. Sher, and A. B. Chen, Phys. Rev. B **33**, 1026 (1986).
[20] D. A. Papaconstantopoulos, *Handbook of the Band Structure of Elemental Solids* (Plenum, New York, 1986).
[21] J. C. Slater and G. F. Koster, Phys. Rev. **94**, 1498 (1954).
[22] L. F. Mattheiss, Phys. Rev. B **2**, 3918 (1970).
[23] P. Vogl, H. P. Hjalmarson, and J. D. Dow, J. Phys. Chem. Solids **44**, 365 (1981).
[24] W. A. Harrison, *Electronic Structure and the Properties of Solids* (Freeman, San Francisco, 1980).
[25] *Landolt-Bornstein: Numerical Data and Functional Relationships in Science and Technology, Group III*, edited by O. Madelung (Springer, Berlin, 1982), Vol. 22.
[26] S. Zollner, J. Appl. Phys. **78**, 5209 (1995).
[27] B. A. Orner, A. Khan, D. Hits, F. Chen, K. Roe, J. Pickett, X. Shao, R. G. Wilson, P. R. Berger, and J. Kolodzey, J. Electron. Mater. **25**, 297 (1996).
[28] B. A. Orner, J. Olowolafe, K. Roe, J. Kolodzey, T. Laursen, J. W. Mayer, and J. Spear, Appl. Phys. Lett. **69**, 2557 (1996).
[29] B. A. Orner, D. Hits, J. Kolodzey, F. J. Guarin, A. R. Powell, and S. S. Iyer, J. Appl. Phys. **79**, 8656 (1996).
[30] P. Boucaud, C. Guedj, D. Bouchier, F. H. Julien, J. M. Lourtioz, S. Bodnar, J. L. Regolini, and E. Finkman, J. Cryst. Growth **157**, (1995).
[31] H. Lee, S. R. Kurtz, J. A. Floro, J. Strane, C. H. Seager, S. R. Lee, E. D. Jones, J. F. Nelson, T. Mayer, and S. T. Picraux, Jpn. J. Appl. Phys. 1 **34**, L1340 (1995).
[32] M. L. Cohen and J. R. Chelikowsky, *Electronic Structure and Optical Properties of Semiconductors* (Springer, Berlin, 1989).
[33] W. Kissinger, M. Weidner, H. Osten, and M. Eichler, Appl. Phys. Lett. **65**, 3356 (1994).
[34] W. Kissinger, H. Osten, M. Weidner, and M. Eichler, Appl. Phys. Lett. **79**, 3016 (1996).
[35] R. A. Soref, Z. Atzman, F. Shaapur, M. Robinson, and R. Westhoff, Opt. Lett. **21**, 345 (1996).
[36] R. Braunstein, A. R. Moore, and F. Herman, Phys. Rev. **109**, 695 (1958).